J. Fluid Mech. (1975), *vol.* 72, *part* 2, *pp.* 269–287
Printed in Great Britain

Thermoconvective instabilities in a horizontal porous layer

By J. P. CALTAGIRONE
Laboratoire d'Aérothermique du C.N.R.S.,
4ter, Route des Gardes, 92190 Meudon, France

(Received 14 March 1975)

Experimental investigations of natural convection in a porous layer placed between two horizontal and isothermal plane surfaces have revealed a new type of convection as the Rayleigh number Ra^* increases: fluctuating convection. A numerical study carried out on a two-dimensional model in order to simulate this phenomenon shows that, apart from the influence of the Rayleigh number, the aspect ratio A (length/height) of a vortical cell is the most important parameter for the occurrence of this type of convection. These quasi-periodic fluctuations induce important variations in the temperature field and in the streamlines. The total heat transport, as defined by the Nusselt number Nu^*, varies within limits which may be separated by 80 % of the mean value. Using the Galerkin method it is possible to deduce the conditions for the onset of convection from a state of pure conduction and also to define the critical conditions for the development of fluctuating convection from another perturbed state. A physical interpretation of the results is given for each type of convection. The results seem to agree with the experimental and numerical results obtained by different authors.

1. Introduction

The first studies of natural convection in a porous medium limited by two isothermal planes maintaining an adverse temperature gradient were carried out by Horton & Rogers (1945) and Lapwood (1948). Lapwood determined the criterion for stability of the conduction state of such a layer and suggested in his linear analysis that convection occurs at Rayleigh numbers above $4\pi^2$.

Experiments have been made by numerous authors in order to check this criterion: Katto & Masuoka (1967), Schneider (1963), Combarnous (1970), Bories (1970) and Cloupeau & Klarsfeld (1970). Their results have confirmed this critical Rayleigh number for the occurrence of convection. These authors carried out their investigations beyond the critical conditions and pointed out the dominant influence of the Rayleigh number on the temperature field (the larger this parameter, the more distorted the isotherms) and on the total heat transport as characterized by the Nusselt number. The relation between the Nusselt and Rayleigh numbers essentially depends on the ratio of the thermal conductivities of the solid–liquid mixture. For this reason, Combarnous & Bories (1973) have

developed a numerical model which takes into account these effects associated with the heat transport between the saturating fluid and the porous layer, the range of investigation there being limited to Rayleigh numbers lower than 400.

Some experiments (Combarnous & Le Fur 1969; Caltagirone, Cloupeau & Combarnous 1971) have revealed another mode of convection, characterized by instabilities in the region of highest temperature gradient, when convection is very important and the Rayleigh number is about 7 times the critical value for occurrence of natural convection (200–390). This phenomenon was first observed in cells of great extent (side length/layer height). However, experiments carried out with cells with sides larger than their heights have also shown that these fluctuations are two-dimensional (Caltagiron 1971). A film prepared with this type of quasi-two-dimensional cell shows the dynamics of these instabilities.

Theoretical interpretations have been given by Busse & Joseph (1972) and Gupta & Joseph (1973), who considered previous work on the Bénard problem (Howard 1963) to determine the critical conditions for the occurrence of these instabilities as well as the variations in the Nusselt number with the Rayleigh number.

Straus (1974), using a series development of the temperature and the stream function, showed that for $Ra^* < 380$ stable two-dimensional convection can exist, while above this value there are always unstable phenomena. A numerical study of this problem developed by Horne & O'Sullivan (1974) for two sets of boundary conditions supports the observations of fluctuating phenomena in a Hele Shaw cell. The qualitative similarity of these results to those found by the author (1974) in his systematic study of stability as a function of the aspect ratio should be noted. In order to define the critical conditions for the occurrence of fluctuating convection as well as the main parameters controlling these instabilities two methods of investigation are discussed in this paper.

(i) The equations for natural convection are solved after having been transformed into difference equations over a rectangular two-dimensional network. The investigation covers the range $Ra^* = 10$–2000 with the aspect ratio (width/height) varying from 0·10 to 4.

(ii) The Galerkin method used to solve any eigenvalue problem is applied to the equations corresponding to a disturbed state. This method enables us to locate the points of appearance of these instabilities in the thermoconvective cell.

2. Formulation of the problem

Consider a saturated porous layer of permeability K, porosity ϵ and height H subject to a temperature gradient ΔT and dynamic pressure p. The saturating fluid has thermal expansion coefficient α, heat capacity $(\rho c)_f$ and coefficient of kinematic viscosity ν. The porous medium is treated as a fluid of thermal conductivity λ^* and heat capacity $(\rho c)^*$, so that at a given point, solid and liquid have the same temperature (a more detailed description of the phenomenon is given by Combarnous & Bories 1973).

Some simplifying hypotheses have been made: that the saturating liquid and

the porous layer are incompressible and that the physical properties of the medium are independent of the temperature. Variations in density with temperature are neglected except in the buoyancy term (Boussinesq's approximation).

The equations for natural convection are written as

$$\rho(\mathbf{V}_{,t}+(\mathbf{V}.\nabla)\,\mathbf{V}) = -\nabla p+\rho\mathbf{g}-(\rho\nu/K)\,\mathbf{V}, \tag{1}$$

$$\rho = \rho_0[1-\alpha(T-T_0)], \tag{2}$$

$$\nabla.\mathbf{V} = 0, \tag{3}$$

$$(\rho c)^* T_{,t} = \lambda^*\nabla^2 T-(\rho c)_f\nabla.(\mathbf{V}T). \tag{4}$$

Using dimensionless parameters (represented by the same symbols) with H for the length scale, $(\rho c)^* H^2/\lambda^*$ for the time scale, ΔT for the temperature scale and $\lambda^*/H(\rho c)_f$ for the velocity scale, we get for a two-dimensional problem the reduced equations

$$M\omega_{,t} = -\nabla.(\omega\mathbf{V})-Pr^* F(Ra^* T_{,x}+\omega), \tag{5}$$

$$\omega = -\nabla^2\psi, \tag{6}$$

$$T_{,t} = \nabla^2 T-\nabla.(\mathbf{V}T), \tag{7}$$

with

$$\boldsymbol{\omega} = (0,\omega,0) = \nabla\times\mathbf{V}, \quad \mathbf{g} = (0,0,-g), \quad \mathbf{V} = (V_x,0,V_z) = (-\psi_{,z},0,\psi_{,x}),$$

where ψ is the stream function. Expressions (5)–(7) include the Rayleigh number $Ra^* = g\alpha(\rho c)_f\Delta THK/\nu\lambda^*$, the Prandtl number $Pr^* = \nu(\rho c)_f/\lambda^*$ and two numbers describing the porous medium: $M = (\rho c)_f/(\rho c)^*$ and $F = H^2/K$. For the media commonly encountered or used by different experimenters F lies between 10^5 and 10^7, making negligible the other terms in (5). Some numerical studies have shown, furthermore, that even large variations in F do not affect the results very much.

There appears from these equations to be a close relation between the temperature and the vorticity, especially in the time derivatives $T_{,t}$ and $\omega_{,t}$. But these partial derivatives have very different orders of magnitude: $\omega_{,t}$ is very much larger than $T_{,t}$, so that in the energy equation the term $T_{,t}$ is sufficient alone for a solution of the system as a function of time, the velocities being at any time those corresponding to the temperature field.

On the other hand, as the Reynolds number based on the mean pore radius is less than 10 in most cases, the energy term in (5) may be neglected. Consequently, the above considerations lead to a new formulation of the system using Darcy's law for flows in porous media:

$$\nabla^2\psi-Ra^* T_{,x} = 0, \tag{8}$$

$$\nabla^2 T-\nabla.(\mathbf{V}T) = T_{,t}. \tag{9}$$

Apart from some attempts to evaluate the influence of F, only these equations in finite-difference form have been solved, for a two-dimensional range.

3. Numerical solution

The solution domain is a rectangle of height H and width L. An important parameter is defined by these two dimensions: the aspect ratio $A = L/H$. Setting $x' = xHA$ and $z' = zH$ the geometrical characteristics of the range become dimensionless. x' varies from 0 to L, z' from 0 to H, x and z from 0 to 1. Equations (8) and (9) then become

$$(A^{-2}\psi_{,xx} + \psi_{,zz}) - A^{-1}Ra^*T_{,x} = 0, \tag{10}$$

$$(A^{-2}T_{,xx} + T_{,zz}) - (V_x A^{-1}T_{,x} + V_z T_{,z}) = T_{,t}, \tag{11}$$

with

$$V_x = -\psi_{,z}, \quad V_z = A^{-1}\psi_{,x}. \tag{12}$$

The boundary conditions assigned to the model may be of one of several types: Dirichlet, Neumann or Fourier. As most experiments have been made with quasi-isothermal surfaces, we shall consider in this study only boundary conditions of Dirichlet type. The horizontal boundaries are isothermal and impermeable, the lateral surfaces adiabatic and impermeable. The cell thus defined is supposed to reproduce a particular thermoconvective roll in a layer of infinite extent. The (accurate) boundary conditions are then written as

$$\begin{aligned}
&\psi = 0, \quad T = 1 \quad \text{for} \quad z = 0 \quad \text{for all } x,\\
&\psi = 0, \quad T = 0 \quad \text{for} \quad z = 1 \quad \text{for all } x,\\
&\psi = 0, \quad T_{,x} = 0 \quad \text{for} \quad x = 0, 1 \quad \text{for all } z.
\end{aligned}$$

The initial conditions concern the temperature field. A consistent distribution of the form $\alpha \cos n\pi x \sin m\pi z$ (where α is an amplification coefficient and m and n wavenumbers) is introduced into the calculation.

The network superposed on the physical domain and representing the geometrical discretization is chosen according to the Rayleigh number. The higher the Rayleigh number, the finer the network for the temperature and velocity gradients, increasing in some parts of the cell. In practice a network with 33×33 nodes is chosen for a Reylaigh number less than or equal to 100 and a network with 49×49 nodes above 100.

Expression (10), which is an elliptical equation of Poisson type, is expressed in finite-difference form and solved by the method of alternating directions. This method is well known and will not be described here. For a given temperature field the second term in (10) is calculated and a convergent iterative process enables us to calculate the stream function for each node and therefore the corresponding velocity field.

The parabolic equation (11) is also solved using the method of alternating directions, but contrary to the solution of (10), in which a simulated time was used to obtain a convergent solution, the time is here physical time and the time step must be chosen according to the phenomenon studied. This energy equation is correctly solved by means of an iterative calculation with the same time step because its second term also includes the temperature. The second term in (10) is calculated from the initial temperature distribution and (10) is solved to determine the stream function. Velocities deduced from this computation are

introduced into the second term in (11), which gives a new temperature field. The cycle is then repeated at the next time step. For each time step we determine the heat transport for all horizontal lines of the network by means of the expression

$$Nu^* = \lambda_{\text{conv}}/\lambda^* = \int_0^1 (T_{,z} + V_z T)\, dx.$$

The total Nusselt number is obtained by taking the average. The calculation is continued until a result independent of the prescribed initial conditions is obtained. The number of iterations varies from 100 to 1000 depending on the regime encountered. Tests are introduced to stop the calculation in the case of convergence. The computing time for a given Rayleigh number and aspect ratio and for a network of 49×49 nodes is about 2 s per iteration using an IBM 370-168 computer. The isotherms and streamlines are traced for each time step from the temperature field and stream-function distribution and then reproduced by a Benson-tracer. Using a fine network (49×49 nodes) as well as a small time increment it is easy to reach a Rayleigh number as large as 2000. The aspect ratios studied vary from 0·1 to 4.

4. Results

Numerical results for natural convection in a horizontal porous layer are reproduced in figure 1 (Nusselt number Nu^* *vs.* aspect ratio A) and show different types of evolution according to the values of the Rayleigh number Ra^* and the cell aspect ratio A. For a given Rayleigh number three types of convection are successively observed as A increases.

(i) For small values of A we note a behaviour corresponding to range I in the plot of aspect ratio *vs.* Rayleigh number (figure 2).

(ii) As A increases the solution tends to a solution corresponding to stable natural convection (range II).

(iii) For still larger values of A, fluctuating convection takes place: range III.

Range I. The perturbation introduced by initial conditions in the form of sinusoidal waves decreases and the system tends to the pure conduction solution: the temperature distribution is a linear function of z, the velocities are zero and the Nusselt number is unity. The further the point is from the curve of marginal stability, the faster this conduction regime is reached. The absolute minimum of this curve is equal to $Ra^* = 4\pi^2$ and occurs for $A = 1$.

The curve of marginal stability found numerically follows very well the variation with A of the critical Rayleigh number for the onset of convection which is given by the linear stability theory developed by Lapwood (1948). For two-dimensional rolls this theory yields a critical $Ra^* = (n^2\pi^2 + \alpha^2)^2/\alpha^2$ with $\alpha = \pi m/A$, where m is the number of rolls in the cell (of aspect ratio A) and n the mode of instability desired. The perturbation introduced to evaluate the stability criterion has the form $\sin n\pi z$. In fact, only the first mode ($n = 1$) has a physical reality: the critical Rayleigh number corresponding to the successive modes can only be verified from a stable conduction state, but this is impossible for $n > 1$ because of the development of convection due to the first mode.

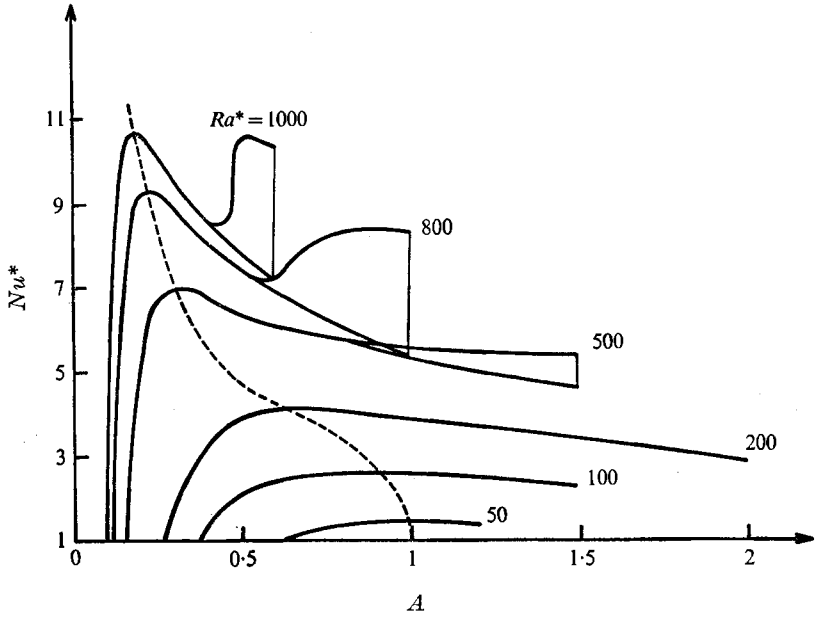

FIGURE 1. Numerical results: variation of the Nusselt number Nu^* as a function of the aspect ratio A for various values of the Rayleigh number Ra^*.

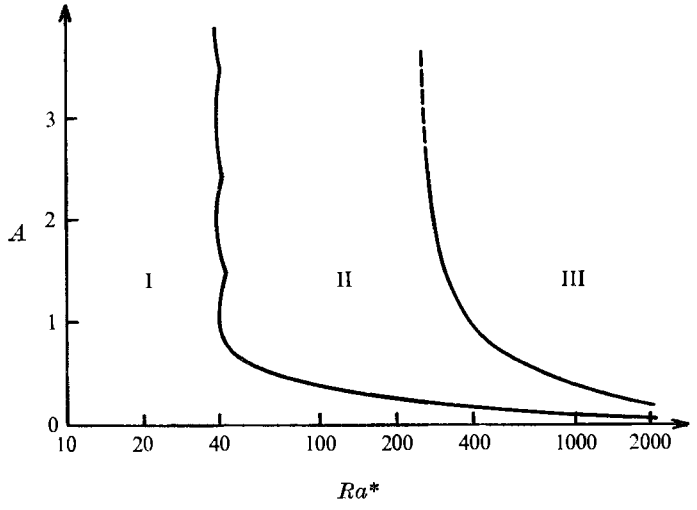

FIGURE 2. Aspect ratio *vs.* Rayleigh number, showing three types of evolution: range I, conduction; range II, stable convection; range III, fluctuating convection.

The curve of marginal stability plotted in figure 2 shows the first mode with the number of rolls per cell corresponding to the minimal Ra^* value (Beck 1972). For large values of the aspect ratio the numerical model generates or eliminates convective rolls in order to return to the condition of Ra^* minimal. It is of interest to note that for $Ra^* \simeq 1000$ natural convection occurs for a cell aspect ratio of about 0·1.

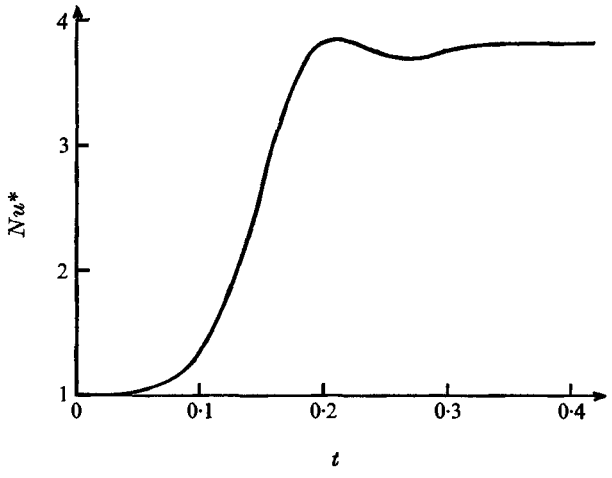

FIGURE 3. Variation of the Nusselt number Nu^* as a function of time during calculation for a Rayleigh number of 200 and an aspect ratio of 0·8.

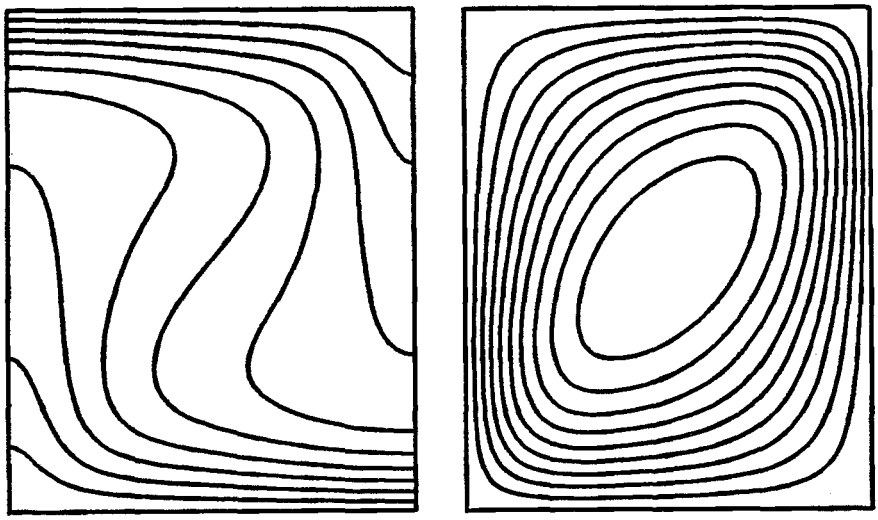

FIGURE 4. (*a*) Temperature field and (*b*) streamlines corresponding to a Rayleigh number of 200 and an aspect ratio of 0·8.

Range II. Beyond the curve of marginal stability the initial perturbation develops to give a stable convergent solution which does not depend on the intensity or nature of this perturbation. The result of a calculation corresponding to this type of evolution ($Ra^* = 200$, $A = 0{\cdot}8$) is shown in figure 3, in which the Nusselt number Nu^* is plotted as a function of time.

Within this range of stable convection the Nusselt number increases, passes through zero then again decreases as A increases (figure 1). This minimum moves towards small aspect ratios as the Rayleigh number increases, thus

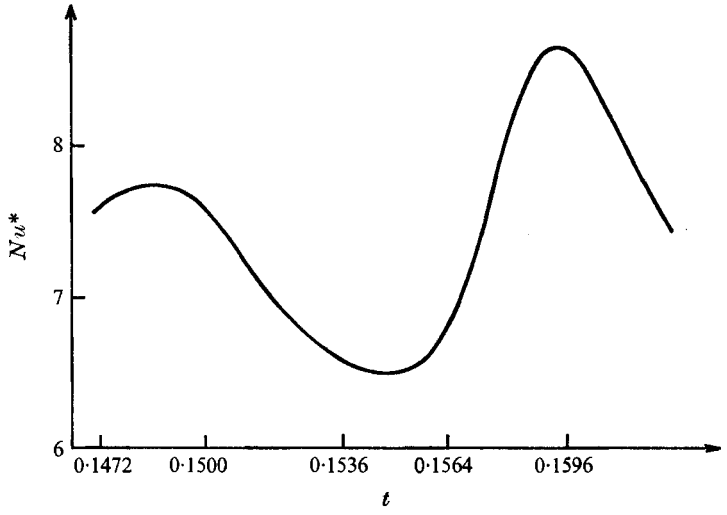

FIGURE 5. Variation of the Nusselt number as a function of time for a Rayleigh number $Ra^* = 800$ and $A = 0{\cdot}8$.

confirming the numerical results found by other authors: Combarnous (1970) for a porous layer and Moore & Weiss (1973) for a fluid layer. Figure 4 shows as an example the temperature field and streamlines for $Ra^* = 200$ and $A = 0{\cdot}8$. The initial system is already strongly perturbed and a gradient opposite to the initial one even appears in the middle of the cell. The strong temperature gradients seem moreover to be located on the lower and upper sides of the rectangle, the centre being filled with a quasi-isothermal core. The higher the Rayleigh number, the more pronounced are these phenomena.

Range III. This range is characterized by the fact that a stable regime cannot be reached. The temperature field, the filtration velocities and the Nusselt number fluctuate with time whatever the number of iterations in the calculation. However, the evolution may sometimes have a quasi-periodic character when the effects of the initial conditions have disappeared. Figure 5 shows the variation of Nu^* as a function of time for a cycle of evolution corresponding to the temperature field and streamlines shown in figure 6.

The types of evolution observed, characterized by different configurations of the temperature field and streamlines, differ considerably, especially for large Rayleigh numbers. For comparatively moderate Rayleigh numbers lying between 300 and 800 and aspect ratios such that the point (Ra^*, A) in figure 2 is not too far from the curve delimiting ranges II and III the temperature and velocity fields are perturbed by instabilities arising near the middles of the cell sides (figure 6). These microvortices develop and are simultaneously carried away by the mainstream. When conditions of instability are reached two new vortices arise, giving the phenomenon a periodic character. Figure 6 shows the different phases of such a cycle for $Ra^* = 800$ and $A = 0{\cdot}8$. For Ra^* values of order 1000 and relatively small values of A a new configuration is observed: four counter-rotating vortices varying around a mean position are found to coexist

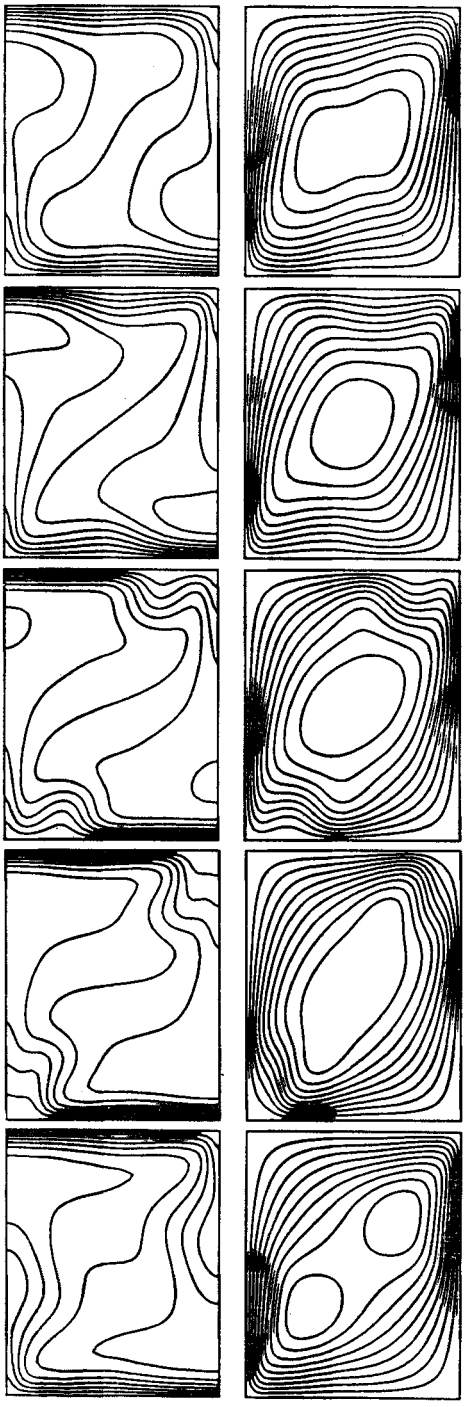

FIGURE 6. Variation of (*a*) the temperature field and (*b*) the streamlines during a cycle. The Rayleigh number is equal to 800 and the aspect ratio to 0·8.

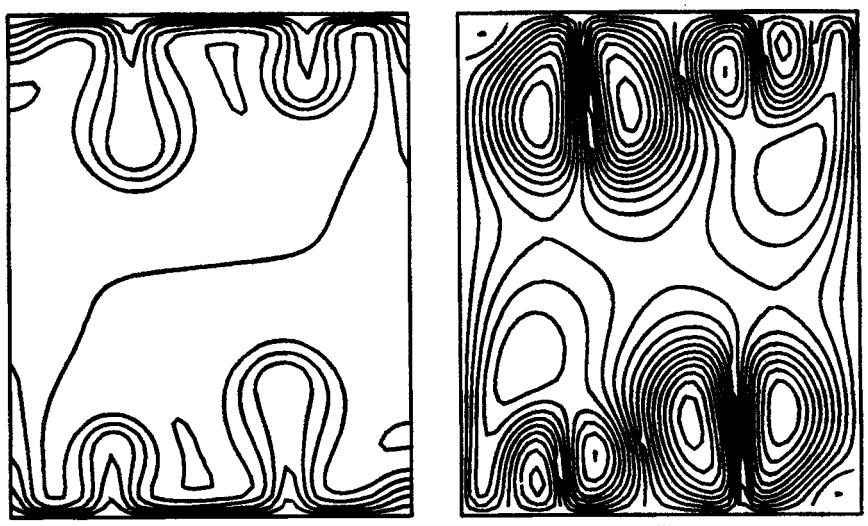

(a) (b)

FIGURE 7. (a) Temperature field and (b) streamlines corresponding to a Rayleigh number of 1000 and an aspect ratio of 0·8.

Ra^*	A	Network	Stable Nu^*	Fluctuating Nu^* (max, min)	Stable ψ (max)
10	1	24 × 24	1·000	—	0·0
$4\pi^2$	1		1·000	—	0·0
50	0·4	32 × 32	1·000	—	0·0
	0·5		1·000	—	0·0
	0·6		1·000	—	0·0
	0·7		1·220	—	1·199
	0·8		1·342	—	1·620
	1		1·450	—	2·112
	1·2		1·386	—	2·131
100	0·1	32 × 32	1·000	—	0·0
	0·2		1·000	—	0·0
	0·3		1·000	—	0·0
	0·4		1·426	—	1·462
	0·5		2·136	—	2·800
	0·6		2·482	—	3·684
	0·8		2·677	—	4·784
	0·9		2·676	—	5·126
	1		2·651	—	5·377
	1·2		2·544	—	5·658
	1·5		2·314	—	5·677
	2		1·853	—	4·783
200	0·1	48 × 48	1·000	—	0·0
	0·2		1·000	—	0·0
	0·3		2·541	—	2·690
	0·4		3·783	—	4·704
	0·5		4·026	—	5·996
	0·6		4·027	—	6·918
	0·8		3·941	—	8·180
	1		3·813	—	8·942
	1·5		3·381	—	9·654
	2		2·914	—	9·380

TABLE 1. Numerical results: Nusselt number Nu^*, maximum value ψ_{max} of the stream function for different values of the Rayleigh number Ra^* and of the aspect ratio A.

Ra^*	A	Network	Stable Nu^*	Fluctuating Nu^* (max, min)	Stable ψ (max)
250	0·4	48 × 48	4·558	—	5·846
	0·6		4·499	—	8·105
	0·8		4·355	—	9·438
	1		4·199	—	10·253
	1·50		3·731	—	11·097
	2		3·250	—	10·977
300	0·3	48 × 48	4·662	—	4·845
	0·4		5·145	—	6·828
	0·5		5·016	—	8·152
	0·6		4·883	—	9·150
	0·8		4·699	—	10·544
	1		4·523	—	11·405
	1·5		4·032	—	12·390
	2		3·513	—	12·270
500	0·1	48 × 48	1·000	—	0·0
	0·15		1·326	—	1·012
	0·2		5·344	—	4·425
	0·25		6·822	—	6·408
	0·3		7·034	—	7·848
	0·4		6·588	—	9·906
	0·6		5·986	—	12·532
	0·7		5·839	—	13·415
	1		—	5·618, 5·332	—
	1·5		—	5·378, 4·501	—
800	0·05	48 × 48	1·000	—	0·0
	0·1		1·000	—	0·0
	0·15		6·484	—	4·640
	0·17		8·408	—	6·285
	0·2		9·152	—	7·549
	0·3		8·747	—	11·067
	0·4		7·811	—	13·357
	0·5		7·345	—	15·077
	0·6		—	7·231, 6·988	—
	0·8		—	8·361, 6·080	—
	1		—	8·322, 5·390	—
	1·25		—	7·498, 5·352	—
	1·5		—	6·981, 5·317	—
1000	0·02	48 × 48	1·000	—	0·0
	0·03		1·000	—	0·0
	0·05		1·000	—	0·0
	0·1		1·000	—	0·0
	0·15		9·183	—	6·290
	0·2		10·633	—	9·142
	0·25		10·190	—	11·195
	0·3		9·455	—	12·813
	0·4		—	8·473, 8·321	—
	0·5		—	10·361, 7·570	—
	0·6		—	10·198, 7·043	—
	0·8		—	13·810, 4·460	—
2000	0·02	48 × 48	1·000	—	0·0
	0·05		1·000	—	0·0
	0·08		5·300	—	3·400
	0·1		12·470	—	6·920
	0·25		—	28·0, 4·5	—

TABLE 1 (*continued*)

in the cell. For slightly larger values of A four or eight additional rolls may appear in the cell and modify to a great extent the streamlines and isotherms (figure 7). As the aspect ratio increases still further, whatever the Rayleigh number, the calculation generates convective rolls and the system is equivalent to a type of evolution corresponding to the range II of stable phenomena.

The above observations are not exhaustive and the limits between these different configurations are not sharply defined. These fluctuations disturb the temperature field, the streamlines, the filtration velocities and the heat transport between the two isothermal surfaces. The Nusselt number varies within limits whose separation may reach 80% of the mean value. The extremes of the variation in the Nusselt number are marked in figure 1. Table 1 gives the quantitative results of this numerical method.

5. Physical interpretation of the results

The results of this numerical analysis enable us to define the critical conditions for stability of a state of pure conduction as well as to determine the regime of stable convection and, on the other hand, point out the existence of the fluctuating regime. However these results must not delude us. A numerical model could not perfectly reproduce the physical situation, apart from the discretization involved in the equations and in the range to be studied.

(i) The model only considers a cell of definite width, while in experimental devices many thermoconvective vortices interacting with each other exist in the porous layer.

(ii) In an experimental porous layer instabilities are latent and satisfaction of the required conditions is sufficient to make them develop, while in the numerical calculation one must either introduce them in form of quasi-periodic perturbations or wait until errors develop in the round numbers, which may take a good time, especially if the calculation is performed in double precision (17 significant numbers on IBM machines). This remark applies especially to the transition from the conduction state to stable convection. The different types of evolution found can, however, explain some phenomena observed experimentally, in particular fluctuating convection. The experiments carried out on a horizontal porous layer used cells of large horizontal size (Combarnous 1970; Bories 1970; Caltagirone 1971) and their results show only a single fluctuating critical Rayleigh number varying from 200 to 390 according to the experiment. But the numerical analysis shows a noticeable influence of the cell aspect ratio on Ra^*_{cf}.

In the fluctuating regime observed with an experimental quasi-two-dimensional cell (2 cm) instabilities are found to appear in the areas of highest temperature gradient and then to develop and disappear into the main vortex. This behaviour is also found in the numerical calculation. These perturbations may sometimes generate a couple of cells which are inserted between two vortices, causing them to move. In other cases these instabilities develop, inducing the disappearance of the vortices on which they arose. The cell expansion seems to increase under the influence of the small vortices carried away by the mainstream and a couple

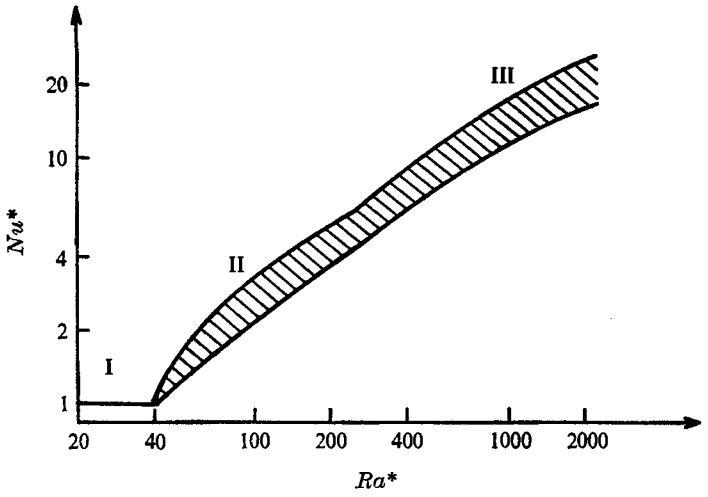

FIGURE 8. Correlation between the Nusselt and Rayleigh numbers found experimentally by various authors: Bories (1970), Combarnous (1970) and Schneider (1963).

of vortices only seem to appear after conditions are met which agree with the results corresponding to range III of figure 2.

The increase in the total heat transport induced by fluctuating phenomena and characterized by a change in the slope in the correlation Nu^* *vs.* Ra^* (figure 8) can be explained by local heat arrival: downflow of cold liquid and upflow of warm liquid as a new pair of vortices appears. The numerical model used gives a correct representation of the behaviour of these thermoconvective vortices, especially for the fluctuating regime. However, this numerical study is in our case more an analysis on an arithmetical computer rather than a theoretical study. For this reason, we now proceed to a study of stability by the Galerkin technique to try to define the conditions for the onset of fluctuating phenomena.

6. Stability

This study has two objects.

(i) The determination of the stability criterion for a porous layer subjected to a constant temperature gradient by using a general method which differs from that developed by Lapwood (1948).

(ii) The determination of the conditions for the occurrence of fluctuating convection by means of the Galerkin method applied to the system of equations describing a state already disturbed by convection (the temperature gradient longer being constant over the height of the layer).

For this purpose we shall consider the system of equations (1)–(4) with the inertial term neglected:

$$\rho \mathbf{V}_{,t} = -\nabla p + \rho \mathbf{g} - (\mu/K)\,\mathbf{V}, \tag{13}$$

$$\nabla . \mathbf{V} = 0, \tag{14}$$

$$\rho = \rho_1[1 - \alpha(T - T_1)], \tag{15}$$

$$\lambda^* \nabla^2 T = (\rho c)_f \nabla . (\mathbf{V}T) + (\rho c)^* T_{,t}. \tag{16}$$

If we introduce small perturbations into Darcy's law (13) of the form

$$T = T_0 + \theta, \quad \mathbf{v} = (u, 0, w) = h(t), \tag{17}$$

$$\mathbf{V} = \mathbf{V}_0 + \mathbf{v}, \quad \mathbf{V}_0 = (V_x, 0, V_z) = \mathbf{f}(x, z), \tag{18}$$

$$p = p_0 + \varpi, \quad T_0 = g(x, z), \tag{19}$$

$$\rho = \rho_0 - \rho_1 \alpha\theta, \tag{20}$$

it then becomes

$$\rho \mathbf{v}_{,t} = -\nabla\varpi + \rho_0 \mathbf{g} - \rho \mathbf{g}\alpha\theta - (\mu/K)(\mathbf{V}_0 + \mathbf{v}). \tag{21}$$

Taking twice the curl of this equation and considering the fact that

$$\nabla \times (\rho \mathbf{g}) = (\mu/K) \nabla \times \mathbf{V}_0$$

gives

$$\partial(\nabla^2 \mathbf{v})/\partial t = \alpha \nabla \times [\nabla \times (\mathbf{g}\theta)] - (\nu/K) \nabla^2 \mathbf{v}, \tag{22}$$

with following components:

$$\partial(\nabla^2 u)/\partial t = -\alpha g \theta_{,xz} - (\nu/K) \nabla^2 u, \tag{23}$$

$$\partial(\nabla^2 w)/\partial t = \alpha g \theta_{,xx} - (\nu/K) \nabla^2 w. \tag{24}$$

Substitution of these small perturbations into the energy equation gives

$$\partial\theta/\partial t = a^* \nabla^2 T_0 + a^* \nabla^2 \theta - M \nabla . (\mathbf{V}_0 T_0) - M \nabla . (\mathbf{v} T_0), \tag{25}$$

with $a^* = \lambda^*/(\rho c)^*$, the thermal diffusivity of the porous medium, and

$$M = (\rho c)_f/(\rho c)^* \quad \text{but} \quad a^* \nabla^2 T_0 = M \nabla . (\mathbf{V}_0 T_0).$$

Hence

$$\partial\theta/\partial t = a^* \nabla^2 \theta - M \nabla . (\mathbf{v} T_0). \tag{26}$$

Considering the z component (24) of (22) and disregarding the second-order term in (26) we obtain the following system:

$$\partial(\nabla^2 w)/\partial t = g\alpha\theta_{,xx} - (\nu/K) \nabla^2 w, \tag{27}$$

$$\partial\theta/\partial t = a^* \nabla^2 \theta - M(u T_{0,x} + w T_{0,z}). \tag{28}$$

With dimensionless variables

$$\theta' = \theta/\Delta T, \quad z' = z/H, \quad t' = t\lambda^*/H^2(\rho c)_f, \quad v' = vH(\rho c)_f/\lambda^*,$$

these equations can be written as

$$(F/Pr^*)\, \partial(w'_{,zz} + w'_{,xx})/\partial t' = Ra^* \theta'_{,xx} - (w'_{,zz} + w'_{,xx}), \tag{29}$$

$$M^{-1} \partial\theta'/\partial t' = (\theta'_{,zz} + \theta'_{,xx}) - (u' T_{0,x} + w' T_{0,z}). \tag{30}$$

We seek solutions of the form

$$\theta' = \theta(z, t) \cos \alpha x, \quad w' = w(z, t) \cos \alpha x, \tag{31), (32}$$

where $\alpha = m\pi/A$. The symbols used here are the same as those used in the numerical study.

The equation of continuity must always be satisfied by the perturbations in the velocity:

$$u'_{,x}+w'_{,z}=0, \quad \text{hence} \quad u'=-\alpha^{-1}Dw\sin\alpha x \quad \text{with} \quad D=d/dz.$$

This finally gives two equations:

$$(F/Pr^*)\,\partial[(D^2-\alpha^2)\,w]/\partial t=-Ra^*\alpha^2\theta-(D^2-\alpha^2)\,w, \tag{33}$$

$$\frac{1}{M}\frac{\partial\theta}{\partial t}=(D^2-\alpha^2)\,\theta-\left(wT_{0,z}-\frac{1}{\alpha}Dw\frac{\sin\alpha x}{\cos\alpha x}T_{0,x}\right). \tag{34}$$

The boundary conditions for the velocity and temperature perturbations are

$$\theta=w=0 \quad \text{for} \quad z=0,1.$$

The Galerkin method used here has been described in the work of Kantorovich & Krylov (1958) or Finlayson (1972).

Let us develop the perturbations in temperature and velocity in the form of series of trial functions satisfying the boundary conditions:

$$\theta(z,t)=\sum_{i=1}^{N}a_i(t)\,\Theta_i(z), \quad w(z,t)=\sum_{i=1}^{N}b_i(t)\,W_i(z). \tag{35}$$

These are introduced into (33) and (34), which are then multiplied by W_j and Θ_j, respectively, and integrated over the height of the layer. Hence

$$(F/Pr^*)\,A_{ij}da_i/dt=Ra^*B_{ij}a_i+C_{ij}b_i, \tag{36}$$

$$M^{-1}D_{ij}db_i/dt=E_{ij}a_i+F_{ij}b_i, \tag{37}$$

with

$$A_{ij}=\int_0^1(D^2W_iW_j-\alpha^2W_iW_j)\,dz.$$

The other matrices are defined in the same way.

Expressed in a matrix form these relations become

$$\mathbf{A}\,d\mathbf{C}/dt=\mathbf{BC},$$

where $\mathbf{A}$ and $\mathbf{B}$ are square matrices, $\mathbf{C}$ the column vector of the coefficients and

$$d\mathbf{C}/dt=\mathbf{A}^{-1}\mathbf{BC}=\mathbf{LC}. \tag{38}$$

In general a phenomenon controlled by a system of linear equations with constant coefficients will remain stable if the roots of the characteristic polynomial are either real and negative or complex with a negative real part.

The solution of the differential system (38) is

$$C_j=c_j\exp(\lambda_jt) \quad (j=1,\ldots,2N). \tag{39}$$

The necessary and sufficient condition for the system to be asymptotically stable is that the eigenvalues of the matrix $\mathbf{L}$ have a negative real part. The characteristic polynomial can be written as follows:

$$\det(\mathbf{L}-\lambda\mathbf{I})=0 \tag{40}$$

($\mathbf{I}$ is the identity operator).

	$N = 1$		$N = 2$	
Trial function	Ra_c^*	α_c	Ra_c^*	α_c
$(1-z)\,z^{2i-1}$	40·000	3·1623	39·937	3·1591
$[(1-z)\,z]\,(2z-1)^{(2i-1)}$	40·000	3·1623	39·479	3·1416
$[(1-z)\,z]^i$	40·000	3·1623	39·479	3·1416
$\sin[(2i-1)\,\pi z]$	39·478	3·1416	—	—

TABLE 2. The critical Rayleigh number and growth rate for the onset of convection calculated using the Galerkin method for four trial functions.

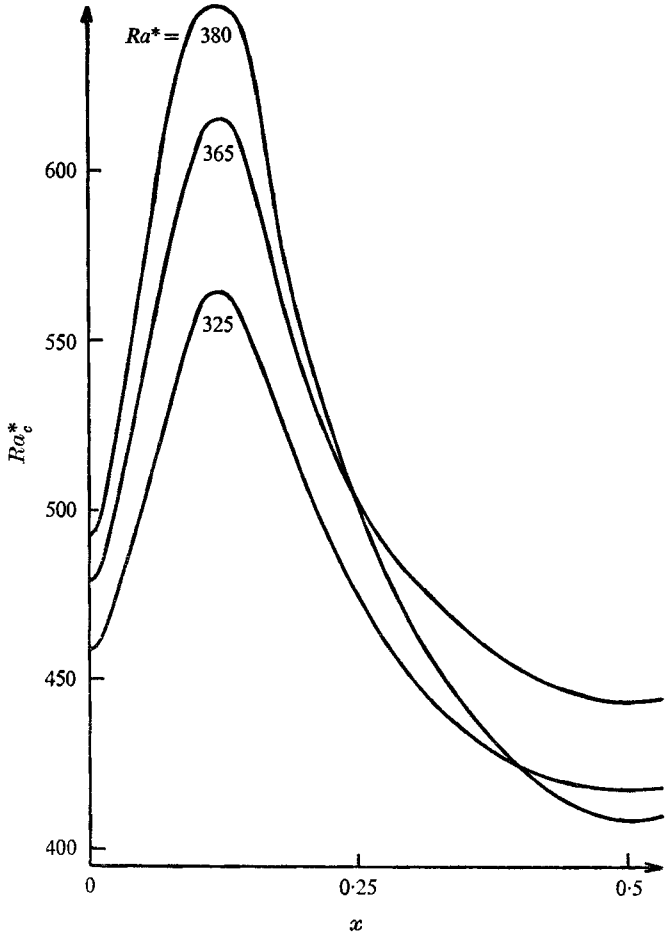

FIGURE 9. Variation of the critical Rayleigh number Ra_c^* as a function of x for different choices of the Rayleigh number.

We have used the Routh–Hurwitz criterion, which gives the necessary and sufficient conditions for all the roots of the characteristic polynomial to have a negative real part. Let us consider only neutral, time-independent evolution, neglecting time-dependent, oscillating evolution. In this case the Routh–

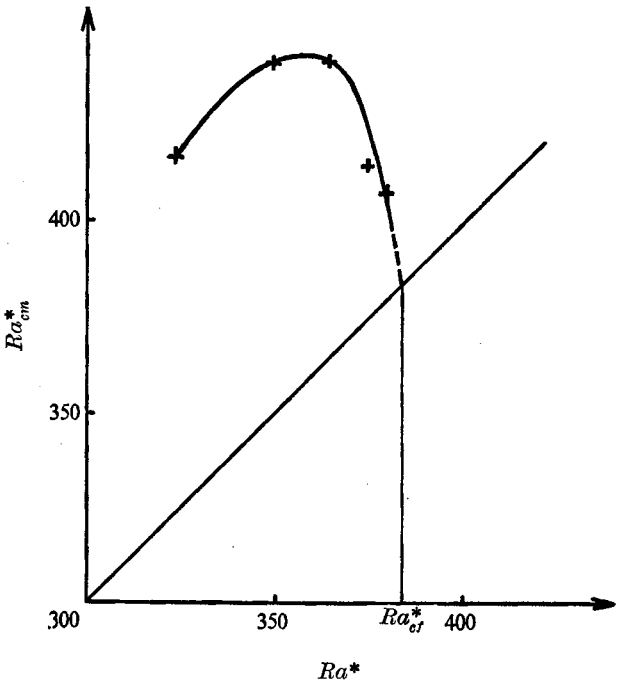

FIGURE 10. The fluctuating critical Rayleigh number obtained by extrapolation of the Ra^*_{cm} curve as a function of Ra^* up to the value $Ra^*_{cm} = Ra^*$.

Hurwitz criterion is equivalent to setting to zero the determinant of the matrix **B** in (38) (Finlayson 1972, p. 150). This condition can be satisfied only for special values of the Rayleigh number corresponding to marginal conditions. As a first step we assign to the terms $T_{0,x}$ and $T_{0,z}$ in (33) the values 0 and 1, respectively, which correspond to the state of pure conduction, and seek the critical Rayleigh number at which convection occurs. The results are given in table 2 for four trial functions satisfying the boundary conditions and for a development (39) limited to the order of 2.

$Ra_c^* = 4\pi^2$ and $\alpha_c = \pi$ are the exact values. The last trial function makes it easy to find these values since it corresponds to the exact solution of the equations used. In a second step the method described above enables us to define the conditions for the appearance of fluctuating natural convection. Fluctuating convection develops only from a stable convection state defined by a temperature field which is known only from experiment or calculation.

The numerical model described in §2 will give complete information for a given Ra^* and aspect ratio A. Consider, for example, an aspect ratio $A = 1$ for a Rayleigh number arbitrarily chosen within the range for stable convection. A numerical calculation gives for some values of x the terms $T_{0,z}$ and $T_{0,x}$ of (34) as a function of z.

At each value of x the stability is studied using the method described above by means of a secondary program which gives the minimal critical Rayleigh number as a function of the wavenumber. The trial functions are chosen under

the assumption that two instabilities given by a function $\sin 2i\pi x$ develop symmetrically with respect to $z = 0{\cdot}5$ over the height of the layer. A critical Rayleigh number $Ra_c^*(x)$ calculated in this manner is higher than the Ra^* value chosen as far as it does not take the critical value. Ra_c^* is plotted as a function of x in figure 9. It can be seen that the minimum in this curve lies at $x = 0{\cdot}5$ and that the corresponding value Ra_{cm}^* is still higher than the Ra^* chosen. The calculation is repeated for several values of Ra^* and the curve reproducing the Ra_{cm}^* values as a function of Ra^* is extrapolated up to the value $Ra_{cm}^* = Ra^*$ (figure 10). For this value of Ra_{cf}^* (in the case of $Ra_{cf}^* = 384 \pm 5$) fluctuating phenomena are found to occur.

It has been noted that near this critical point the calculation becomes less and less convergent; at all higher Ra^* values the numerical calculation is divergent and the stability can no longer be studied.

To sum up, this study of the stability, from an initial state of stable convection, in a porous layer subjected to an adverse gradient shows that (i) the fluctuating critical Rayleigh number $Ra_{cf}^* = 384 \pm 5$ for $A = 1$ agrees with the solution of the numerical problem and (ii) the instabilities are located in the middle of the horizontal sides of the cell, as can be seen in figure 6.

7. Conclusions

The investigations of natural convection to date seem to be motivated by two factors.

(i) A more accurate description of the phenomena with some improvements concerning the heat transport between the fluid and the porous matrix, the variations with temperature of the physical characteristics or the variation with the filtration velocity of the thermal conductivity tensor.

(ii) A study of stability for various geometrical configurations and under different boundary conditions. This study is not limited to the case of porous media and several investigations of the problem of a fluid heated from below have been carried out (Moore & Weiss 1973; Busse 1968).

The purpose of the present study is to contribute to the understanding of the phenomena observed experimentally in a horizontal porous layer in two respects.

(i) The results show that the choice of a numerical two-dimensional model based on experiments in which fluctuating phenomena were observed in cells of small thickness is fully justified. They point out the prevailing influence of the cell aspect ratio for the onset of instabilities. This parameter is generally not actually controlled and varies with time from one vortex to another. If the numerical model used cannot take into account this possibility of variation of A it can show, however, the occurrence of these instabilities, which are the first signs of the appearance or disappearance of a couple of vortices.

(ii) The stability analysis developed here using the Galerkin method enables one to find the conditions for the onset of natural convection: $Ra^* = 4\pi^2$, and also to predict the fluctuating critical Rayleigh number $Ra^* = 384$ for the aspect ratio $A = 1$, a result which agrees very well with the results obtained

with the numerical model. The results discussed here still give a very imperfect reproduction of the facts. A more realistic approach could be made by using a numerical three-dimensional model, in which the reduced height of the layer would be very small compared with the transverse dimensions, and by introducing into the calculation boundary conditions closer to reality.

The author wishes to express his thanks to Professor J. J. Bernard, Director of the Laboratoire d'Aérothermique of the C.N.R.S., for helpful discussions on this study.

REFERENCES

BECK, J. L. 1972 *Phys. Fluids*, **15**, 1377.

BORIES, S. 1970 *Rev. Gen. Therm.* **9**, 1377.

BUSSE, F. H. 1968 *J. Fluid Mech.* **37**, 457.

BUSSE, F. H. & JOSEPH, D. D. 1972 *J. Fluid Mech.* **54**, 521.

CALTAGIRONE, J. P. 1971 *Mém. C.N.A.M., Paris.*

CALTAGIRONE, J. P. 1974 *Comptes Rendus*, **278**, 259.

CALTAGIRONE, J. P., CLOUPEAU, M. & COMBARNOUS, M. 1971 *Comptes Rendus*, **273**, 833.

CHANDRASEKHAR, S. 1961 *Hydrodynamic and Hydromagnetic Stability*. Oxford: Clarendon Press.

CLOUPEAU, M. & KLARSFELD, S. 1970 *Rep. Laboratoire d'Aérothermique.*

COMBARNOUS, M. 1970 *Rev. Gen. Therm.* **9**, 1355.

COMBARNOUS, M. & BORIES, S. 1973 *Int. J. Heat Mass Transfer*, **17**, 505.

COMBARNOUS, M. & LE FUR, B. 1969 *Comptes Rendus*, **269**, 1009.

FINLAYSON, B. A. 1972 *The Method of Weighted Residuals and Variational Principles.* Academic.

GUPTA, V. P. & JOSEPH, D. D. 1973 *J. Fluid Mech.* **57**, 491.

HORNE, R. N. & O'SULLIVAN, M. J. 1974 *J. Fluid Mech.* **66**, 339.

HORTON, C. W. & ROGERS, F. T. 1945 *J. Appl. Phys.* **16**, 367.

HOWARD, L. N. 1963 *J. Fluid Mech.* **17**, 405.

KANTOROVICH, L. V. & KRYLOV, V. I. 1958 *Approximate Methods in Higher Analysis.* Groningen, The Netherlands: Noordhoff.

KATTO, Y. & MASUOKA, T. 1967 *Int. J. Heat Mass Transfer*, **10**, 297.

KLARSFELD, S. 1970 *Rev. Gen. Therm.* **9**, 1403.

LAPWOOD, E. R. 1948 *Proc. Camb. Phil. Soc.* **44**, 508.

MOORE, D. R. & WEISS, N. O. 1973 *J. Fluid Mech.* **58**, 289.

SCHNEIDER, M. J. 1963 *11th Int. Cong. Refrigeration (Munich)*, paper 11-4.

STRAUS, J. M. 1974 *J. Fluid Mech.* **64**, 51.